

Central exclusive production in CMS+TOTEM

Ferenc Siklér^{a,*}

for the CMS and TOTEM Collaborations

^aWigner Research Centre for Physics,
Konkoly-Thege M. út 29-33, 1121 Budapest, Hungary

E-mail: sikler.ferenc@wigner.hu

The central exclusive production of charged hadron pairs in pp collisions at a centre-of-mass energy of 13 TeV is examined, based on data collected in a special high- β^* run of the LHC. Events are selected by requiring both scattered protons detected in the TOTEM Roman pots, exactly two oppositely charged identified particles in the CMS silicon tracker, and the energy-momentum balance of these four particles. The nonresonant continuum processes are studied with the invariant mass of the centrally produced two-pion system in the resonance-free region, $m < 0.7$ GeV or $m > 1.8$ GeV. Differential cross sections as functions of the azimuthal angle between the surviving protons, squared four-momenta, and two-hadron invariant mass are measured in a wide region of scattered proton transverse momenta $0.2 \text{ GeV} < p_{1,T}, p_{2,T} < 0.8 \text{ GeV}$ and for hadron rapidities $|y| < 2$. A rich structure of interactions related to double pomeron exchange emerges. The parabolic minimum in the distribution of the two-proton azimuthal angle is observed for the first time. It can be understood as an effect of additional pomeron exchanges between the protons from the interference between the bare and the rescattered amplitudes. After model tuning, various physical quantities related to the pomeron cross section, proton-pomeron and hadron-pomeron form factors, trajectory slopes and intercepts, as well as coefficients of diffractive eigenstates of the proton are determined.

The European Physical Society Conference on High Energy Physics (EPS-HEP2023)
21-25 August 2023
Hamburg, Germany

*Speaker

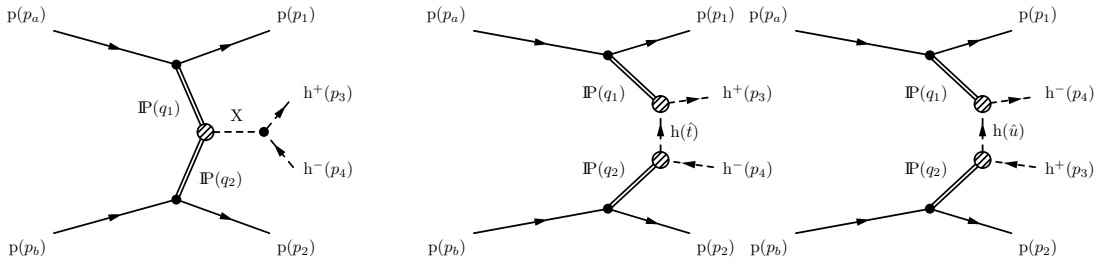


Figure 1: Born-level Feynman diagrams for central exclusive production of hadron pairs via double pomeron exchange, depicting resonant (left) and nonresonant continuum (rightmost two) contributions.

1. Introduction

In collisions of protons, the exclusive central production of a few particles offers a clean laboratory for the study of various phenomena [1]. At high energies, for not too small momentum transfers, these processes are dominated by double pomeron exchange. They provide a gluon rich environment which may lead to the creation of hadrons free of valence quarks, the glueballs.

Born-level Feynman diagrams of processes playing roles in central exclusive production of charged hadron pairs via double pomeron exchange are shown in Fig. 1. We distinguish two main processes. The two pomerons may fuse through a short-lived resonance (X), which in turn decays to a pair of oppositely charged hadrons. Alternatively, the two pomerons may interact via the exchange of a virtual hadron (h), leading to the production of a pair of oppositely charged hadrons in a nonresonant process, the topic of the present study. Both t -channel and u -channel graphs should be taken into account.

Such a simple picture gets complicated when the various effects of suppression, absorption, and other corrections are properly taken into account. Additional pomeron exchanges between the incoming (and outgoing) protons cause interference between the bare and the rescattered amplitudes. The resulting quantity is often referred to as the eikonal survival factor. The interference is expected to lead to interesting diffractive dip phenomena in the angular distributions [2].

2. Data taking and analysis

A detailed description of the CMS detector, together with a definition of the relevant kinematic variables, can be found in Ref. [3]. The TOTEM detector is described in Ref. [4]. The data were taken in a special $\beta^* = 90$ m run of the LHC, in 2018 (β^* is the value of the amplitude function at the collision point). With such a high β^* setting the beam divergence is reduced, hence the forward detectors are able to probe the elastic-scattering regime at small scattering angles and small transverse momenta.

The Roman pots (RPs) measure the direction of the scattered proton. Its transverse momentum is inferred on the assumption that the total momentum of the proton has not changed in the collision. The acceptance of the stations is not azimuthally uniform [4] and the coverage in the transverse momentum of the scattered protons is $0.175 \text{ GeV} < |p_{1/2,y}| < 0.670 \text{ GeV}$. The acceptance maps of the two arms are correlated since signals from both arms are used for triggering. In addition, their

efficiency depends on the individual silicon strip detector efficiencies, which change with time. The silicon tracker covers the region $|\eta| < 3$. This translates into acceptance for centrally produced hadrons for $|y| < y_{\max}$, where $y_{\max} \approx 2.0$ in the case of $\pi^+\pi^-$, and $y_{\max} \approx 1.6$ for K^+K^- and $p\bar{p}$. Tracking is efficient for $p_T > 0.1$ GeV, but the particle identification capabilities are substantially reduced at higher momenta.

For this data set the Level 1 (hardware) trigger requires detected protons in each RP arm, in various configurations. Only the data from double pomeron exchange triggers are used in the analysis, not those from the elastic trigger. The high-level trigger (HLT) has multiple components: the pixel activity and track filters.

The data are studied as functions of the four-momentum transfers squared (t_1, t_2) or equivalently ($p_{1,T}, p_{2,T}$), and the azimuthal angle ϕ between the momentum vectors of the two scattered protons in the transverse plane. The measurement is fully corrected without using Monte Carlo simulations, except those describing low-energy phenomena needed for tracking efficiency correction. The results are corrected for the momentum acceptance and the effect of the elastic trigger veto of the RPs using data, for the local straight track reconstruction efficiency in the RPs, based on the hit structure of each tracklet at the strip level. Data are corrected for trigger, reconstruction, and particle identification efficiencies of the charged hadron pair in the silicon tracker.

The classification of events is largely based on momentum conservation in the transverse plane. Once corrected for the effects of the beam crossing angle, the system of the incoming protons has zero momentum. Therefore, the sum of the momenta of the scattered protons and the other particles created in the collision should also be zero. The momentum conservation in the longitudinal direction is already utilised for the calculation of longitudinal momenta of the scattered protons, since the resolution from a direct measurement would be poor.

3. Results

The measured distributions are the following: distribution of the azimuthal angle ϕ between the scattered proton momenta, $d^3\sigma/dp_{1,T}dp_{2,T}d\phi$; distribution of the two-hadron invariant mass m , $d^3\sigma/dp_{1,T}dp_{2,T}dm$; distribution of the squared four-momentum $\max(\hat{t}, \hat{u})$ of the virtual meson, $d^3\sigma/dp_{1,T}dp_{2,T}d\max(\hat{t}, \hat{u})$, in the range $0.2 < p_{1,T}, p_{2,T} < 0.8$ GeV.

We focus on $\pi^+\pi^-$ production because this system has a wide invariant mass window ($0.35 < m < 0.65$ GeV) without resonance contributions, contrary to the K^+K^- case. A selection of distributions of $d^3\sigma/dp_{1,T}dp_{2,T}d\phi$ as a function of ϕ in several ($p_{1,T}, p_{2,T}$) bins are shown in Fig. 2. The differential cross sections are given in units of $\mu\text{b}/\text{GeV}^2$. Except for the lowest transverse momentum bins, they feature a minimum where the differential cross section gets close to zero, while local maxima at $\phi = 0$ and π are also present. The distributions are asymmetric at low and high transverse momenta, but there exists a symmetric region around $p_{1,T} + p_{2,T} \approx 0.8 - 0.9$ GeV.

The data can be fitted with a simple functional form

$$\frac{d^3\sigma}{dp_{1,T}dp_{2,T}d\phi} = [A(R - \cos \phi)]^2 + c^2, \quad (1)$$

where A , R , and c are functions of ($p_{1,T}, p_{2,T}$). If the total amplitude crosses zero at a given ϕ , its squared value will have a parabolic minimum. Such a dip at $\phi = \arccos R$ can be understood

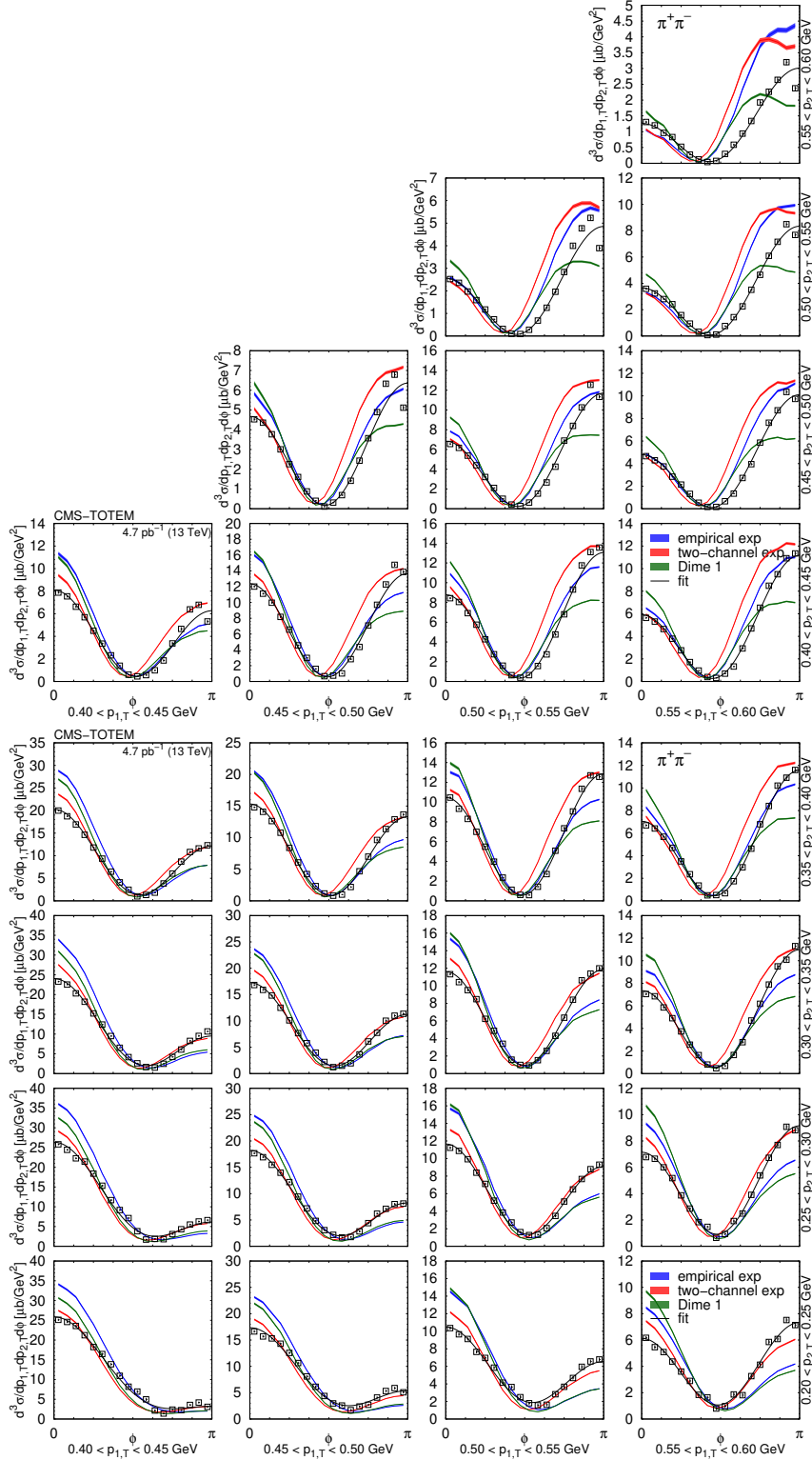


Figure 2: Distribution of $d^3\sigma/dp_{1,T}dp_{2,T}d\phi$ as a function of ϕ in several $(p_{1,T}, p_{2,T})$ bins, in units of $\mu\text{b}/\text{GeV}^2$. Measured values (black symbols) are shown together with the predictions of the empirical and the two-channel models (coloured symbols) using the tuned parameters for the exponential proton-pomeron form factors (see text for details). Curves corresponding to DIME (model 1) are also plotted. Results of fits with the form $[A(R - \cos \phi)]^2 + c^2$ are plotted with curves. The error bars indicate the statistical uncertainties.

as an effect of additional pomeron exchanges between the incoming protons, resulting from the interference between the bare and the rescattered amplitudes [2]. The term containing c is added incoherently, it is small and is present to improve the quality of the fit.

The dependences of the parameters A , R , and c on (t_1, t_2) can be well described though

$$A(t_1, t_2) = 4\sqrt{t_1 t_2} \cdot A_0 e^{b(t_1+t_2)}, \quad c(t_1, t_2) = c_0 e^{d(t_1+t_2)}, \quad (2)$$

$$R(t_1, t_2) \approx \frac{1.2(\sqrt{-t_1} + \sqrt{-t_2}) - 1.6\sqrt{t_1 t_2} - 0.8}{\sqrt{t_1 t_2} + 0.1}. \quad (3)$$

While the parametrisation overall gives a good description of the data, there are some deviations at low and high $-(t_1 + t_2)$ values for A and c , respectively. The fitted values are $A_0 = 10.6 \pm 0.2\sqrt{\text{nb}}/\text{GeV}^3$, $b = 3.9 \pm 0.1 \text{ GeV}^{-2}$, while $c_0 = 2.1 \pm 0.1\sqrt{\text{nb}}/\text{GeV}$, $d = 3.8 \pm 0.1 \text{ GeV}^{-2}$.

4. Model tuning

In the following we will deal with three models (empirical, one-channel, and two-channel), and three parametrisations (exponential, Orear-type, and power-law) of the proton-pomeron form factor. The full list of model parameters can be found in Ref. [5]. In the case of the empirical model the rescattering amplitude comes from a simple parametrisation of the elastic differential proton-proton amplitude, fitted to the measured cross sections. The one-channel model assumes ground state protons (one eigenstate), while the two-channel model works with two diffractive proton eigenstates. DIME [2] (v1.07) is a MC event generator for exclusive meson pair production via double pomeron exchange.

For the tuning of physics parameters the tool PROFESSOR [6] is employed. It parametrises the per-bin generator response to parameter variations and numerically optimises the parameterised behaviour. The χ^2/dof values are in the range 1.6 – 2.0 (empirical), 1.2 – 1.5 (one-channel), and 1.0 – 1.3 (two-channel). Good fits are achieved with the one-channel or the two-channel models using exponential or Orear-type form factors, while the numerically best one is the two-channel model with exponential parametrisation of the proton-pomeron form factor. It is clear that the power-law parametrisation of the proton-pomeron form-factor is disfavoured by our data. The empirical model also has a high goodness-of-fit value, although with fairly few parameters.

The values of the fitted parameters are shown in Fig. 3. In the case of the two-channel model, parameter values of two models describing the elastic differential proton-proton cross section from Ref. [7] are also indicated (DIME 1 and 2). Settings of DIME 1 agree well with the best tuned values of the parameters, with the exception of $\Delta|a|^2$ and $\Delta\gamma$. The extracted values of σ_0 are mostly stable, except for the one-channel exponential case, and disagree with early $C_{\mathbb{P}}$ estimates.

The distributions of $d^3\sigma/dp_{1,T}dp_{2,T}d\phi$ in the nonresonant region ($0.35 < m < 0.65 \text{ GeV}$) as a function of ϕ in several $(p_{1,T}, p_{2,T})$ bins are shown in Fig. 2. Measured values are shown together with the predictions of the empirical and the two-channel models using the tuned parameters for the exponential proton-pomeron form factors. Curves corresponding to DIME (model 1) are also plotted: this generator gives a poor description of the data for $\phi > \pi/2$. While the various tuned models give a much better description, there are some regions with sizeable disagreements pointing to the need for further theoretical developments, specially for low $p_{1,T}$ and low $p_{2,T}$ as well as high $p_{1,T}$ and high $p_{2,T}$ combinations.

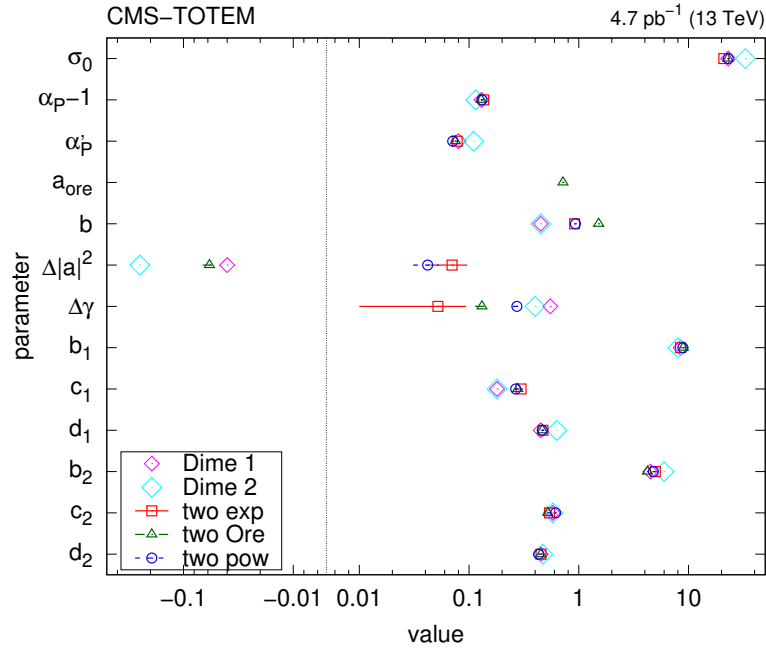


Figure 3: Values of best parameters for the two-channel model with several choices of the proton-pomeron form factor (exponential, Orear-type, power-law). Parameter values of models describing the elastic differential proton-proton cross section from Ref. [7] are also indicated (DIME models 1 and 2).

Further details and all results of the analysis can be found in Ref. [5]. This work was partially supported by the National Research, Development and Innovation Office of Hungary (K 128786).

References

- [1] M. Albrow, T. Coughlin and J. Forshaw, *Central Exclusive Particle Production at High Energy Hadron Colliders*, *Prog. Part. Nucl. Phys.* **65** (2010) 149 [1006.1289].
- [2] L.A. Harland-Lang, V.A. Khoze and M.G. Ryskin, *Modelling exclusive meson pair production at hadron colliders*, *Eur. Phys. J. C* **74** (2014) 2848 [1312.4553].
- [3] CMS collaboration, *The CMS experiment at the CERN LHC*, *JINST* **3** (2008) S08004.
- [4] TOTEM collaboration, *The TOTEM experiment at the CERN Large Hadron Collider*, *JINST* **3** (2008) S08007.
- [5] CMS and TOTEM collaborations, *Nonresonant central exclusive production of charged hadron pairs in proton-proton collisions at $\sqrt{s} = 13$ TeV*, *CMS-PAS-SMP-21-004* (2023).
- [6] A. Buckley, H. Hoeth, H. Lacker, H. Schulz and J.E. von Seggern, *Systematic event generator tuning for the LHC*, *Eur. Phys. J. C* **65** (2010) 331 [0907.2973].
- [7] V. Khoze, A. Martin and M. Ryskin, *Diffraction at the LHC*, *Eur. Phys. J. C* **73** (2013) 2503 [1306.2149].